Direct Measurements of Field-Dependent Ordering in a Low-Field Vortex Glass State

Frederick S. Wells, Alexey V. Pan, X. Renshaw Wang, Igor A. Golovchanskiy, Sergey A. Fedoseev, Hans Hilgenkamp, and Anatoly Rozenfeld

***Abstract*—The variation of topological defect density and hexatic order parameter were measured over a range of micro-Tesla fields in a 2-D superconducting vortex glass. This was achieved through scanning SQUID microscopy of the vortex distribution in $YBa_2Cu_3O_{7-\delta}$ thin films under field-cooled conditions. It was discovered that, although the defect density decreased for increasing magnetic fields, giving the impression of a more lattice-like vortex distribution, the hexatic order parameter also decreased, showing that the distribution was less orientationally ordered.**

***Index Terms*—Flux pinning, scanning probe microscopy, superconducting thin films, yttrium barium copper oxide.**

I. Introduction

GLASS-LIKE distributions of vortices in type II superconductors have been a subject of intense interest in recent years [1], [2], in both the two-dimensional (thin film) [3] and three dimensional (bulk) [4] cases.

Most studies into vortex glass behavior involve measurement or simulation of macroscopic quantities such as transport current and sample magnetization to determine transitions in the vortex phase diagram [3], [4]. Analyses of the properties of vortex glass states by direct measurement are less common, but may provide a more fundamental understanding of the nature of these distributions of vortices [5].

In the absence of defects or thermal fluctuations, the distribution of vortices in a superconductor would be a regular triangular lattice with sixfold rotational symmetry. In this perfect lattice each vortex has six nearest neighbors. However, in reality even highly ordered vortex distributions in the lattice state possess topological defects, which can be dislocations (positional defects) or disclinations (orientational defects) [6], [7]. Ryu and Stroud identify a disclination in the vortex lattice as a vortex having a number of nearest neighbors other than 6, and a dislocation as a pair of adjacent disclinations with one having more nearest neighbors and one having less [7].

The vortex glass state is highly non-regular and dominated by such defects. Superconducting phase diagrams often show a rich variety of glass-like states with complex transition lines [1], [3], [4]. However, in this two-dimensional study we consider only the differences between a hexatic vortex glass, in which a sixfold orientational order is maintained, and an isotropic vortex glass, in which it is not [1], [4], [7].

In our previous work [5], $YBa_2Cu_3O_{7-\delta}$ (YBCO) thin films under very low field conditions were directly observed and analyzed using Scanning Superconducting Quantum Interference Device (SQUID) microscopy (SSM) [8], [9], and the vortices were found to be in an isotropic vortex glass state. Glass states such as these are expected to dominate the phase diagram in YBCO thin films grown by pulsed laser deposition (PLD) due to the high number of strong pinning sites [10]–[13].

The present work explores the field dependence of properties relating to order in this glassy state. The properties considered are the distribution of the number of neighbors to each vortex, and the hexatic order parameter. We find that the modal number of nearest neighbors is six for all fields studied, but that the proportion of vortices having six nearest neighbors increases with increasing applied field.

We also find that the angular distribution of vortices becomes less regular for higher fields in the observed field range, as evidenced by a decreasing hexatic order parameter.

II. Experimental Details

$YBa_2Cu_3O_{7-x}$ films with thickness close to 200 nm were grown by pulsed laser deposition [14]–[16] on STO substrates, and lithographically patterned into 3×3 mm squares. One film was selected, with critical temperature $T_c = 90.0 \pm 0.5$ K and the critical current density $J_c \simeq 1.5 \times 10^{10}$ A/m^2 at $T = 77$ K

Manuscript received August 23, 2015; accepted February 19, 2016. Date of publication February 23, 2016; date of current version March 14, 2016. This work was supported in part by the Australian Research Council and in part by the University of Wollongong.

F. S. Wells and A. V. Pan are with the Institute for Superconducting and Electronic Materials, University of Wollongong, Wollongong, NSW 2522, Australia (e-mail: fsw793@uowmail.edu.au; pan@uow.edu.au).

X. R. Wang is with the Faculty of Science and Technology and MESA+ Institute for Nanotechnology, University of Twente, 7500 AE Enschede, The Netherlands, and also with Electrochemical Energy Laboratory, Massachusetts Institute of Technology, Cambridge, MA 02139 USA.

I. A. Golovchanskiy is with the Institute for Superconducting and Electronic Materials, University of Wollongong, Wollongong, NSW 2522, Australia, with the Laboratory of Topological Quantum Phenomena in Superconducting Systems, Moscow Institute of Physics and Technology, State University, Dolgoprudny, Moscow Region, 141700 Moscow, Russia, and also with the Laboratory of Superconducting Metamaterials, National University of Science and Technology MISIS, 119049 Moscow, Russia.

S. A. Fedoseev is with the Institute for Superconducting and Electronic Materials, University of Wollongong, Wollongong, NSW 2522, Australia, and also with Center for Medical Radiation Physics, University of Wollongong, Wollongong, NSW 2522, Australia.

H. Hilgenkamp is with the Faculty of Science and Technology and MESA+ Institute for Nanotechnology, University of Twente, 7500 AE Enschede, The Netherlands.

A. Rozenfeld is with the Center for Medical Radiation Physics, University of Wollongong, Wollongong, NSW 2522, Australia.

Color versions of one or more of the figures in this paper are available online at http://ieeexplore.ieee.org.

Digital Object Identifier 10.1109/TASC.2016.2533570

and applied magnetic field $B_a \to 0$ T, as measured using a Quantum Design MPMS magnetometer.

The selected YBCO film was field cooled to a stable 4.2 K using a helium bath cryostat. Field-cooling was repeated for several applied field values in the low field vortex-glass region of the phase diagram (between 0.05 and 5.47 μT). A single high-resolution scan of the vortex distribution was taken at each field using the scanning SQUID microscopy (SSM) technique described in [5]. The SQUID loop has size 3 μm $\times$ 5 μm, and nominal scan height of 5 μm.

Supercurrent in the samples was calculated from the resulting SSM images using an inverse Biot-Savart law procedure [9], [22]–[25].

The position of vortices in SSM images was determined programmatically using a particle detection algorithm to give an array of spatially distributed vortex locations. Delaunay triangulation was applied to the vortex positions to determine the number of nearest neighbors to each vortex and the bond angle of each of these neighbors.

Delaunay triangulation is a mathematical procedure mapping the distribution of vortices in space to a network of non-overlapping triangles. Each triangle has a vortex at each corner and has edges connecting nearest-neighboring vortices.

From this triangulation the number of nearest neighbors to each vortex was determined for all internal vortices. Where internal vortices are defined as all vortices excluding those at the edges of the measured area or at the sample edge, as well as their nearest neighbors.

The hexatic order parameter (HOP) was also determined for each vortex distribution. The HOP is given by $|\psi_6|^2$, where:

$$\psi_6 = \frac{1}{N_{\text{int}}} \sum_i \frac{1}{n(i)} \sum_j e^{6i\theta_{ij}} \tag{1}$$

Here, N_{int} is the number of internal vortices, $n(i)$ is the number of nearest neighbors to a vortex i, θ_{ij} is the angle between nearest-neighboring vortices i and j relative to a fixed axis.

A regular triangular vortex lattice (as expected for a defect-free superconducting sample) has a sixfold rotational symmetry and hence has hexatic order parameter $|\psi_6|^2 = 1$. Any deviation from the regular lattice reduces the HOP to a value between 1 and 0.

III. Results

Scanning SQUID images were obtained after field cooling at several field values in the specified range. Fig. 1 gives typical magnetic field data at a particular field value.

The light region is the superconducting sample, with dark spots showing vortex positions. The dark area at the left is outside the sample. The vortices in this image appear larger than their actual size, and show an apparent asymmetry due to the scan height and angle of the SQUID magnetometer [5].

Supercurrent calculated in the film from similar SSM images is shown in Fig. 2, for scans taken with different field histories.

Vortices are seen here as dark spots since no current flows in the vortex core, with bright circulating currents around. Shielding currents are also seen at the sample edge, especially in the lower-field images.

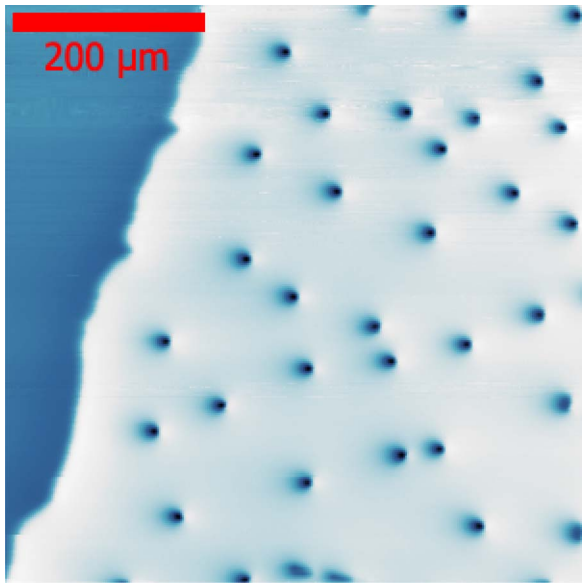

Fig. 1. Scanning SQUID image of vortices near the edge of a YBCO film after field cooling at 1.47 μT. The brightness of each pixel represents the strength of magnetic field at the corresponding point on the sample. Shading on the left of each dark vortex is due to a small tilt of the SQUID pick-up loop relative to the sample surface.

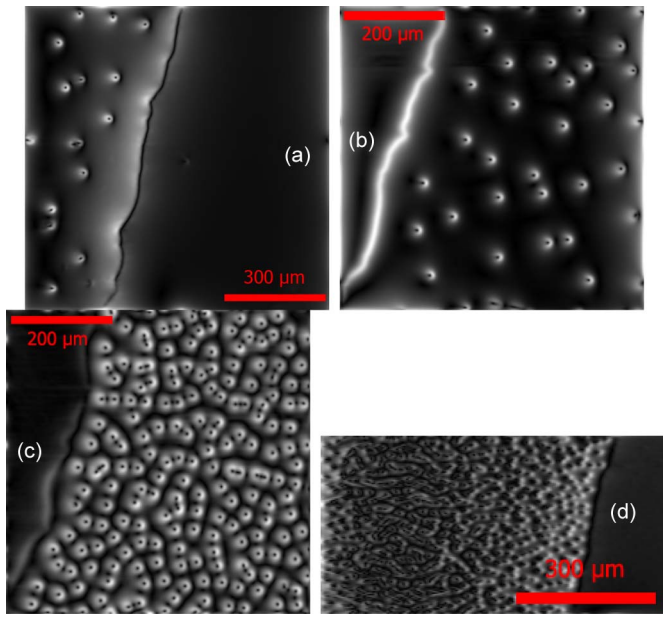

Fig. 2. Supercurrent in YBCO film after field cooling at (a) 0.05, (b) 1.47, (c) 2.10, and (d) 5.46 μT, calculated from Scanning SQUID images. Brighter regions represent higher currents.

Delaunay triangulation was applied successfully to the vortex positions from scanning SQUID data at each field, as shown in Fig. 3.

The number of nearest neighbors to each vortex was calculated by defining nearest-neighboring vortices as those connected in the same triangle by the triangulation algorithm. That is, any three vortices through which a circle can be drawn which encompasses no other vortices are defined to be neighbors.

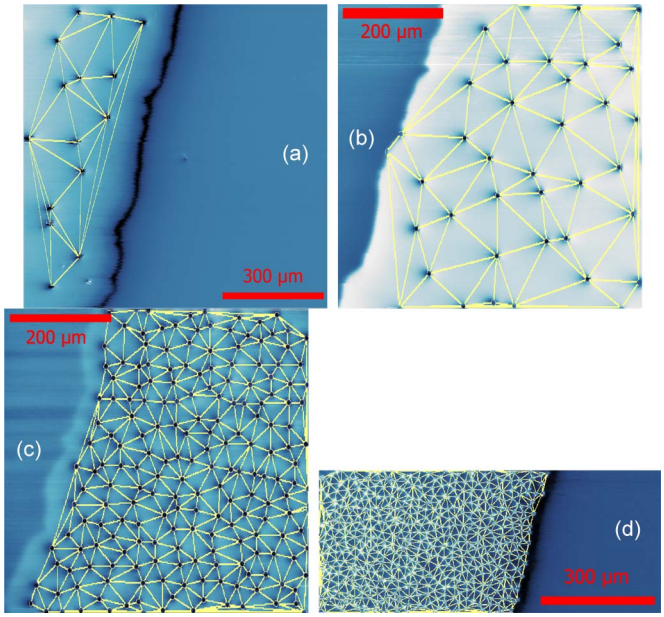

Fig. 3. Delaunay triangulation mapped onto scanning SQUID images at (a) 0.05, (b) 1.47, (c) 2.10, and (d) 5.46 μT. The triangulation is represented by lines connecting each detected vortex position to its neighbors.

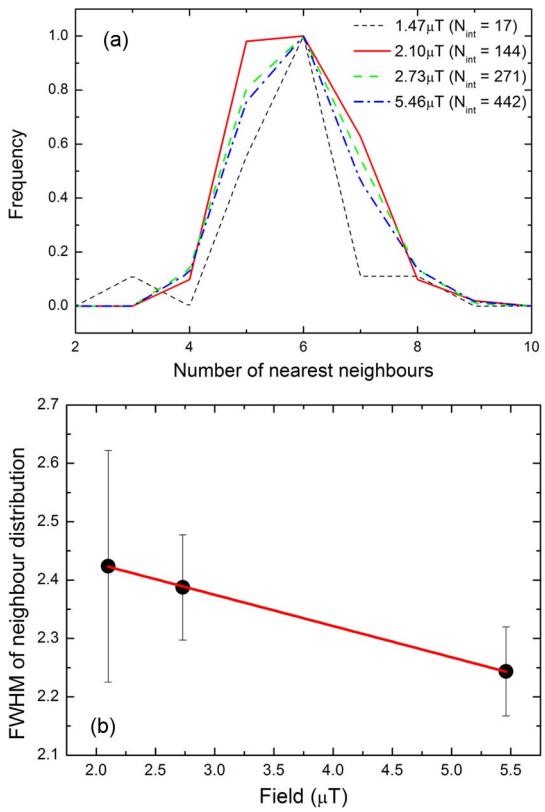

Fig. 4. (a) Normalized occurrence of the number of nearest neighbors to vortices in the SSM scans at various fields. The total number of internal vortices (N_{int}) counted for each field is given in the legend. (b) Plot of the width of the Gaussian fit to these curves against applied field. An error-weighted linear trend line is plotted with gradient $(-5.353 \pm 0.077) \times 10^4$ T^{-1}.

The distribution of the number of nearest neighbors to each internal vortex at a particular field is shown in Fig. 4(a). A normalized Gaussian fit is plotted for each distribution, with the total number of counted vortices (N_{int}) indicated for each. The SSM scan at 0.05 μT is excluded since $N_{\mathrm{int}} = 0$ for this scan. The 1.47 μT scan is shown, but excluded from further analysis due to statistical inaccuracy resulting from low vortex count.

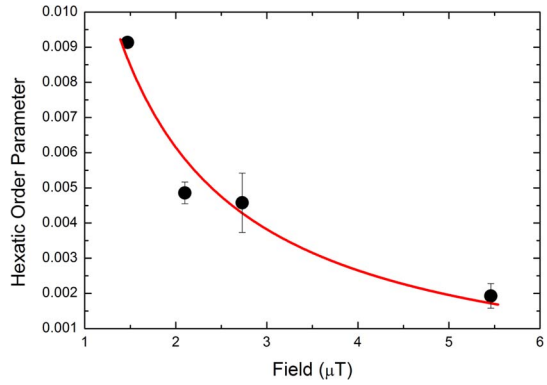

Fig. 5. Variation of the hexatic order parameter $|\psi_6|^2$ of vortex distribution with applied field. Error bars reflect the accuracy of identification of vortex positions. The hyperbolic fit gives $1/|\psi_6|^2 = B \times (9.99 \pm 0.74) \times 10^7$ T^{-1}.

The full width at half maximum (FWHM) of these fit curves represents the spread of the number of nearest neighbors. This width is plotted against field in part (b) of this figure. Error bars represent standard error in the Gaussian fit, which naturally decreases when a larger number of vortices are counted. It is found that the FWHM decreases linearly with applied field, but with relatively low gradient. This indicates that for higher fields a greater proportion of vortices have six nearest neighbors, and hence that the number of topological defects (as defined above) slightly decreases with field in the range measured.

The angle between vortices is also measured from the Delaunay triangulation, and this is used to calculate the hexatic order parameter for each field value used. The HOP is plotted against field in Fig. 5. The error ranges for HOP are calculated from an estimation of the error in distinguishing closely spaced vortices in each image, as explained below.

It is seen that the HOP decreases with increasing field in an inversely proportional manner. This implies that the angles between vortices become less regular for increasing field in the field range studied.

IV. Discussion

As field increases, the topological defect density decreases, making the vortex distribution slightly resemble more a regular lattice. This was expected, since the sample is in the low-field (re-entrant) vortex glass region of the phase diagram, and an increase in field moves the sample closer to the vortex lattice region [2] by increasing the influence of vortex-vortex repulsion.

However, if the distribution were simply becoming more lattice-like with increasing field, the hexatic order parameter would also increase with field. Instead, HOP was found to be inversely proportional to applied field. This shows that while the number of topological defects decreases with increasing field, the angle between vortices is less regular and orientational order is overall decreased.

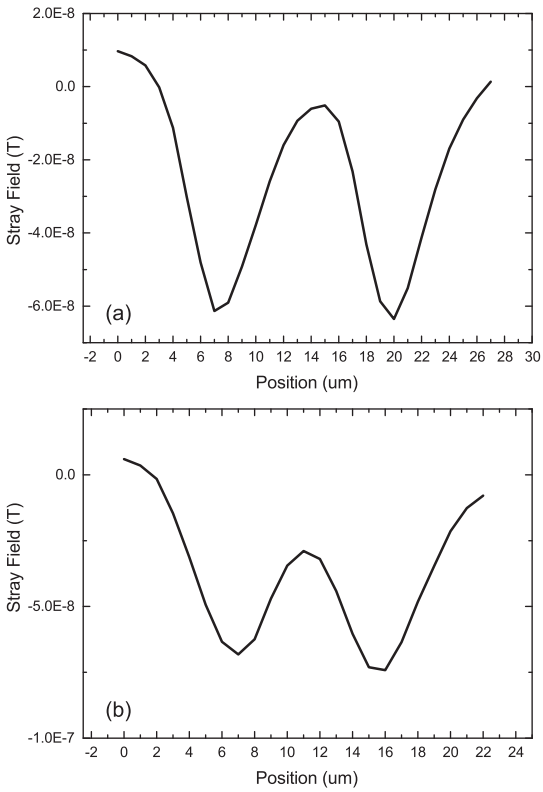

Fig. 6. Field profiles across closely paired vortices showing (a) no stray field overlap at 13-μm separation and (b) half-height overlap at 9-μm separation, which may result in a failure to interpret these as separate vortices.

As mentioned previously, significant spread of the magnetic stray field occurs between the sample surface and the scan height, increasing the apparent size of vortices. This can lead to difficulty in distinguishing vortices from their neighbors when intervortex distance is small, leading to error. Several groups of vortices with apparent overlap are seen in Fig. 7.

To investigate this, linear profiles of measured field were plotted across pairs of closely spaced vortices in the 5.46 μT scan. Fig. 6 shows the profiles of pairs of vortices at 13 μm and 9 μm separation, showing that the stray fields from vortices closer than about 10 μm overlap so as to give no point of zero measured field between the vortices.

This overlap causes errors in the analysis of these vortices, most significantly that the particle detection algorithm may falsely recognize two closely-spaced vortices as a single vortex. This then causes error in the number of nearest neighbors to this and surrounding vortices, as well as the angles between these vortices. Both of these errors will in turn affect the hexatic order parameter.

The particle detection parameters were optimized for each vortex distribution independently in order to avoid such errors, and the Delaunay triangulation was visually examined for false vortex positions after each attempt. By this process all of the distributions were mapped with a high degree of accuracy, except for the 2.73 μT scan, which had lower quality as reflected by the large error bar in Fig. 5.

This scan does however show one interesting feature not seen in other scans: a linear region of notably increased vortex

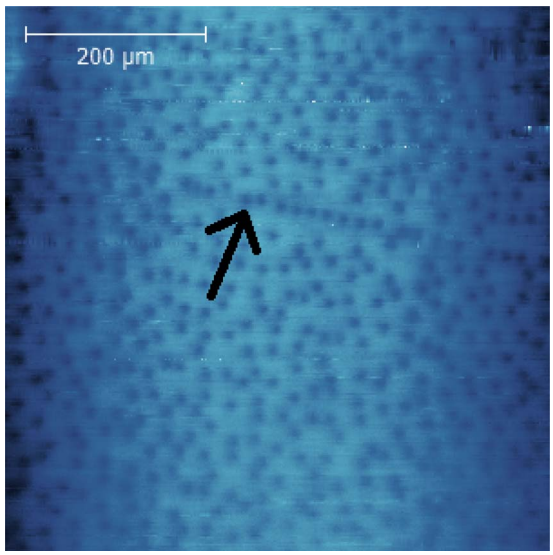

Fig. 7. Scanning SQUID image of vortices in the YBCO film after field cooling at 2.73 μT, showing the presence of a linear defect, as indicated by the arrow.

density with length at least 400 μm, as shown in Fig. 7. This high-density region was seen to be reproduced upon heating above T_c and re-cooling, implying that it is a linear defect with width of the order of the size of vortices or smaller. This may be caused by substrate twinning, an extended grain boundary, or micro-mechanical damage to the sample.

This defect is not seen in other scans as they were taken at different positions on the sample.

V. Conclusion

We have directly examined the field dependence of the ordering of vortices in the low-field vortex glass state in a YBCO thin film, as observed by scanning SQUID microscopy of field-cooled states. Ordering of the vortex glass was quantified using two parameters: the spread of the number of nearest neighbors to each vortex, and the hexatic order parameter.

It was found that the distribution of nearest neighbors peaked at six for all fields studied. With increasing field, the relative number of topological defects was seen to reduce, but this did not increase the orientational order. Instead, the hexatic order parameter decreased with increasing field.

If the current study were extended to higher fields, we expect that the vortex distribution would transition into the lattice state at some well-defined point [25], [26]. The hexatic order parameter would be expected to reach a minimum before increasing sharply at the vortex glass-lattice transition, while the number of topological defects would decrease steadily before sharply dropping at this transition point [7]. The HOP and nearest neighbor distribution may also vary with field in the vortex lattice regime, and may have different field dependences in the high-field vortex glass phase and in other glass-like phases.

Direct measurements of field-dependent vortex ordering in other regions of the phase diagram may prove to be a very exciting avenue for future research. However, such studies should consider larger areas and hence larger vortex numbers for heightened statistical significance.

REFERENCES

[1] T. Natterman and S. Scheidl, "Vortex-glass phases in type-II superconductors," *Adv. Phys.*, vol. 49, no. 5, pp. 607–704, Jul. 2000.

[2] D. S. Fisher, M. A. Fisher, and D. A. Huse, "Thermal fluctuations, quenched disorder, phase transitions, and transport in type-II superconductors," *Phys. Rev. B, Condens. Matter Mater. Phys.*, vol. 43, no. 1, pp. 130–159, Jan. 1991.

[3] M. Shahbazi *et al.*, "Vortex-glass phase transition and enhanced flux pinning in C^{4+}-irradiated $BaFe_{1.9}Ni_{0.1}As_2$ superconducting single crystals," *Supercond. Sci. Technol.*, vol. 26, no. 9, Aug. 2013, Art. no. 095014.

[4] D. J. Bishop, L. Gammel, C. A. Murray, D. B. Mitzi, and A. Kapitulnik, "Observation of an hexatic vortex glass in flux lattices of the high-T_c superconductor $Bi_{2.1}Sr_{1.9}Ca_{0.9}Cu_2O_{8+\delta}$," *Phys. Rev. Lett.*, vol. 169, no. 19, pp. 72–79, May 1991.

[5] F. S. Wells, A. V. Pan, X. R. Wang, S. A. Fedoseev, and H. Hilgenkamp, "Analysis of low-field isotropic vortex glass containing vortex groups in $YBa_2Cu_3O_{7-x}$ thin films visualized by scanning SQUID microscopy," *Sci. Rep.*, vol. 5, p. 8677, 2015.

[6] E. Kröner and K.-H. Anthony, "Dislocations and disclinations in material structures: The basic topological concepts," *Annu. Rev. Mater. Sci.*, vol. 5, pp. 43–72, Aug. 1975.

[7] S. Ryu and D. Stroud, "First-order melting and dynamics of flux lines in a model for $YBa_2Cu_3O_{7-\delta}$," *Phys. Rev. B, Condens. Matter Mater. Phys.*, vol. 54, no. 2, pp. 1320–1333, Jul. 1996.

[8] J. R. Kirtley and J. P. Wikswo, Jr., "Scanning SQUID microscopy," *Annu. Rev. Mater. Sci.*, vol. 29, pp. 117–148, 1999.

[9] A. Sugimoto, T. Yamaguchi, and I. Iguchi, "Supercurrent distribution in high-T_c superconducting $YBa_2Cu_3O_{7-y}$ thin films by scanning superconducting quantum interference device microscopy," *Appl. Phys. Lett.*, vol. 77, no. 19, pp. 3069–3071, Nov. 2000.

[10] A. Nandgaonkar, D. G. Kanhere, and N. Trivedi, "Competition between columnar pins and vortex screening: A doubly reentrant phase diagram," *Phys. Rev. B, Condens. Matter Mater. Phys.*, vol. 66, no. 10, Sep. 2002, Art. no. 104527.

[11] V. Pan *et al.*, "Supercurrent transport in $YBa_2Cu_3O_{7-\delta}$ epitaxial thin films in a dc magnetic field," *Phys. Rev. B, Condens. Matter Mater. Phys.*, vol. 73, no. 5, Feb. 2006, Art. no. 054508.

[12] A. V. Pan, S. V. Pysarenko, and S. X. Dou, "Quantitative description of critical current density in YBCO films and multilayers," *IEEE Trans. Appl. Supercond.*, vol. 19, no. 3, pp. 3391–3394, Jun. 2009.

[13] I. A. Golovchanskiy, A. V. Pan, O. V. Shcherbakova, and S. A. Fedoseev, "Rectifying differences in transport, dynamic, and quasi-equilibrium measurements of critical current density," *J. Appl. Phys.*, vol. 114, no. 16, Oct. 2013, Art. no. 163910.

[14] I. A. Golovchanskiy, A. V. Pan, S. A. Fedoseev, and M. Higgins, "Significant tunability of thin film functionalities enabled by manipulating magnetic and structural nano-domains," *Appl. Surf. Sci.*, vol. 311, pp. 549–557, 2014.

[15] A. V. Pan, S. Pysarenko, and S. X. Dou, "Drastic improvement of surface structure and current-carrying ability in $YBa_2Cu_3O_7$ films by introducing multilayered structure," *Appl. Phys. Lett.*, vol. 88, no. 23, Jun. 2006, Art. no. 232506.

[16] A. V. Pan, S. V. Pysarenko, D. Wexler, S. Rubanov, and S. X. Dou, "Multilayering and Ag-doping for properties and performance enhancement in $YBa_2Cu_3O_7$ films," *IEEE Trans. Appl. Supercond.*, vol. 17, no. 2, pp. 3585–3588, Jun. 2007.

[17] A. V. Pan *et al.*, "Thermally activated depinning of individual vortices in $YBa_2Cu_3O_7$ superconducting films," *Phys. C, Supercond.*, vol. 407, no. 1/2, pp. 10–16, Aug. 2004.

[18] A. V. Pan and S. X. Dou, "Comparison of small-field behavior in MgB_2, Low- and high-temperature superconductors," *Phys. Rev. B, Condens. Matter Mater. Phys.*, vol. 73, no. 5, Feb. 2006, Art. no. 052506.

[19] Y. Tsuchiya, Y. Nakajima, and T. Tamegai, "Development of surface magneto-optical imaging method," *Phys. C, Supercond.*, vol. 470, no. 20, pp. 1123–1125, Nov. 2010.

[20] V. M. Pan and A. V. Pan, "Vortex matter in superconductors," (Russian), *Fiz. Niz. Temp.*, vol. 27, no. 9/10, pp. 991–1011, 2001.

[21] V. M. Pan and A. V. Pan, "Vortex matter in superconductors," *Low Temp. Phys.*, vol. 27, no. 9, pp. 732–746, Sep. 2001.

[22] C. Jooss *et al.*, "Magneto-optical studies of current distributions in high-T_c superconductors," *Rep. Prog. Phys.*, vol. 65, no. 5, pp. 651–788, May 2002.

[23] F. S. Wells, "Magneto-optical imaging and current profiling on superconductors," Honours Thesis, School Physics Inst. Supercond. Electron. Mater., Univ. Wollongong, Wollongong, NSW, Australia, 2011.

[24] F. S. Wells *et al.*, "Dynamic magneto-optical imaging of superconducting thin films," *Supercond. Sci. Technol.*, vol. 29, no. 3, Feb. 2016, Art. no. 035014.

[25] B. J. Roth, N. G. Sepulveda, and J. P. Wiskwo, Jr., "Using a magnetometer to image a two-dimensional current distribution," *J. Appl. Phys.*, vol. 65, no. 1, pp. 361–372, Jan. 1988.

[26] A. V. Pan and P. Esquinazi, "The Labusch parameter of a driven flux line lattice in $YBa_2Cu_3O_7$ superconducting films," *Eur. Phys. J. B*, vol. 17, no. 3, pp. 405–410, Oct. 2000.

[27] A. V. Pan and P. Esquinazi, "Influence of a driving force on the pinning of a field-cooled vortex lattice," *Phys. C, Supercond.*, vol. 341–348, pp. 1187–1188, Nov. 2000.